

Electric-field-induced phase transition in $\langle 001 \rangle$ -oriented $\text{Pb}(\text{Mg}_{1/3}\text{Nb}_{2/3})\text{O}_3$ - PbTiO_3 single crystals

This article has been downloaded from IOPscience. Please scroll down to see the full text article.

2002 J. Phys.: Condens. Matter 14 L571

(<http://iopscience.iop.org/0953-8984/14/29/103>)

View [the table of contents for this issue](#), or go to the [journal homepage](#) for more

Download details:

IP Address: 171.66.16.96

The article was downloaded on 18/05/2010 at 12:16

Please note that [terms and conditions apply](#).

LETTER TO THE EDITOR

Electric-field-induced phase transition in $\langle 001 \rangle$ -oriented $\text{Pb}(\text{Mg}_{1/3}\text{Nb}_{2/3})\text{O}_3\text{--PbTiO}_3$ single crystals

Ke-Pi Chen¹, Xiao-Wen Zhang¹ and Hao-Su Luo²

¹ State Key Lab. of New Ceramics and Fine Processing, Department of Materials Science and Engineering, Tsinghua University, Beijing 100084, People's Republic of China

² State Key Lab. of High Performance Ceramics and Superfine Microstructure, Shanghai Institute of Ceramics, Chinese Academy of Sciences, Shanghai 201800, People's Republic of China

E-mail: chenkepi99@mails.tsinghua.edu.cn

Received 12 April 2002

Published 11 July 2002

Online at stacks.iop.org/JPhysCM/14/L571

Abstract

$\langle 001 \rangle$ -oriented $0.7\text{Pb}(\text{Mg}_{1/3}\text{Nb}_{2/3})\text{O}_3\text{--}0.3\text{PbTiO}_3$ single crystals were poled under two different electric fields, $E_{\text{poling}} = 4$ and 13 kV cm^{-1} . In addition to the temperature-dependent dielectric constant measurement, x-ray diffraction was also used to identify the poling-induced phase transitions. The results showed that the phase transition significantly depends on the poling intensity. The weaker field ($E_{\text{poling}} = 4 \text{ kV cm}^{-1}$) was able to overcome the effect of the random internal field to produce the phase transition from the rhombohedral ferroelectric state with short-range ordering (microdomains), FE_{SRO} , to the rhombohedral ferroelectric state with long-range ordering (macrodomains), FE_{LRO} . But the rhombohedral ferroelectric-to-tetragonal ferroelectric phase transition originating from $\langle 111 \rangle$ to $\langle 001 \rangle$ polarization rotation could only be induced by the stronger field ($E_{\text{poling}} = 13 \text{ kV cm}^{-1}$). The sample poled at $E_{\text{poling}} = 4 \text{ kV cm}^{-1}$ showed a higher piezoelectric constant, $d_{33} > 1500 \text{ pC N}^{-1}$, than the sample poled at $E_{\text{poling}} = 13 \text{ kV cm}^{-1}$.

It was observed about 20 years ago that $\text{Pb}(\text{Zn}_{1/3}\text{Nb}_{2/3})\text{O}_3\text{--PbTiO}_3$ (PZN–PT) single crystals with compositions close to the morphotropic phase boundary (MPB) exhibited anomalously large piezoelectric and electromechanical coupling constants, particularly when the samples were poled along $\langle 001 \rangle$ axes [1, 2]. But this did not attract much attention until several stimulating papers appeared in 1997 [3–6]. Recently, both theoretical and experimental results have provided a better understanding of the abnormal properties of single-crystal PZN–PT and $\text{Pb}(\text{Mg}_{1/3}\text{Nb}_{2/3})\text{O}_3\text{--PbTiO}_3$ (PMN–PT) in the MPB region. Fu and Cohen [7] pointed out that a large piezoelectric response could be driven by polarization rotation induced by an external electric field in these single crystals. At almost the same time, Noheda *et al*

[8–10] used synchrotron x-ray powder diffraction measurements to reveal the existence of a monoclinic phase between the previously established tetragonal and rhombohedral regions in $\text{Pb}(\text{Zr}, \text{Ti})\text{O}_3$ (PZT) which further supports the concept of polarization rotation. Subsequently, similar experiments were carried out on PZN–PT and PMN–PT single crystals [11–14], and it was found that monoclinic (FE_M) and orthorhombic (FE_O) phases can also be induced in a narrow range of compositions with appropriate poling history. But the rhombohedral phase FE_R may also rotate to a tetragonal phase, FE_T , under an external electric field via an alternative path, which is different from that in PZT.

Only a few published papers have focused on the phase transition behaviour and piezoelectric response of $\langle 001 \rangle$ -poled PMN–PT single crystals with composition close to the MPB. On the basis of measurements of the temperature dependence of the dielectric constant of a poled $\langle 001 \rangle$ -oriented 0.7PMN–0.3PT single crystal, Viehland *et al* [15] suggested that the transition from a normal ferroelectric state (macrodomains) to a relaxor state (microdomains) with increasing temperature is responsible for the secondary transformation near 90°C . For a poled $\langle 001 \rangle$ -oriented 0.67PMN–0.33PT single-crystal sample, Lu *et al* [16] also found an additional ferroelectric phase transition (FE–FE) at 80°C using dielectric constant measurements. But they were uncertain whether this phase change corresponds to a FE_O – FE_T or a FE_R – FE_O transition.

In this letter it is shown that the phase transition of poled $\langle 001 \rangle$ -oriented 0.7PMN–0.3PT single crystals depends significantly on the intensity of the poling field. Dielectric constant measurements indicate that in addition to a transition at $T_{max} = 147^\circ\text{C}$, there is a second phase transition far below T_{max} . X-ray diffraction experiments reveal that the crystalline state of the field-induced transition depends on the poling history of the crystal.

Single crystals of 0.7PMN–0.3PT were grown by the modified Bridgman method described in [17]. It was reported that segregation behaviour during the crystal growth results in compositional inhomogeneities of the PMN–PT single crystals even in the same boule [17]. Thus, the composition of the specimen was identified using x-ray fluorescence analysis to make sure that it is 0.7PMN–0.3PT. In this study, only one $\langle 001 \rangle$ -oriented $5 \times 10 \times 0.5 \text{ mm}^3$ specimen was used in all experiments to keep the composition unchanged. The sample was electroded with silver paste and poled at room temperature under various electrical fields (first cycle: 4 kV cm^{-1} ; second cycle: 13 kV cm^{-1}). The dielectric constant was measured as a function of temperature at a heating rate of 4°C min^{-1} using an HP4192A Precision LCR meter at different frequencies (0.1, 1, and 10 kHz). XRD experiments were performed on a Rigaku D/max-3B diffractometer using $\text{Cu K}\beta$ monochromatic radiation ($\lambda = 1.39223 \text{ \AA}$). The piezoelectric constants (d_{33}) of the samples exposed to the different poling fields were measured using a Berlincourt-type quasistatic d_{33} -meter.

Figures 1(a)–(c) show the dielectric constants plotted as a function of temperature for unpoled (figure 1(a)) and poled $\langle 001 \rangle$ -oriented samples (figure 1(b), $E_{poling} = 4 \text{ kV cm}^{-1}$ and (c), $E_{poling} = 13 \text{ kV cm}^{-1}$) at different frequencies under zero-field heating (ZFH). For the unpoled sample, only one phase transition occurred, at 147°C , and the dielectric constant ϵ showed weak frequency dependence. This can be attributed to a phase transition between a cubic state and a rhombohedral ferroelectric state with short-range ordering (microdomains), FE_{SRO} . In contrast with the case for the unpoled sample, both poled samples, with $E_{poling} = 4$ and 13 kV cm^{-1} , demonstrate a field-induced secondary transition around 90°C , as shown in figures 1(b) and (c).

It is difficult to discern the difference between the secondary transitions in figures 1(b) and (c) by means of dielectric constant measurements. But the XRD patterns of these two samples are quite different. Figure 2(a) shows the (004) diffraction line ($2\theta = 87.50^\circ$) of the unpoled sample. This symmetric profile has a relatively wide FWHM (full width

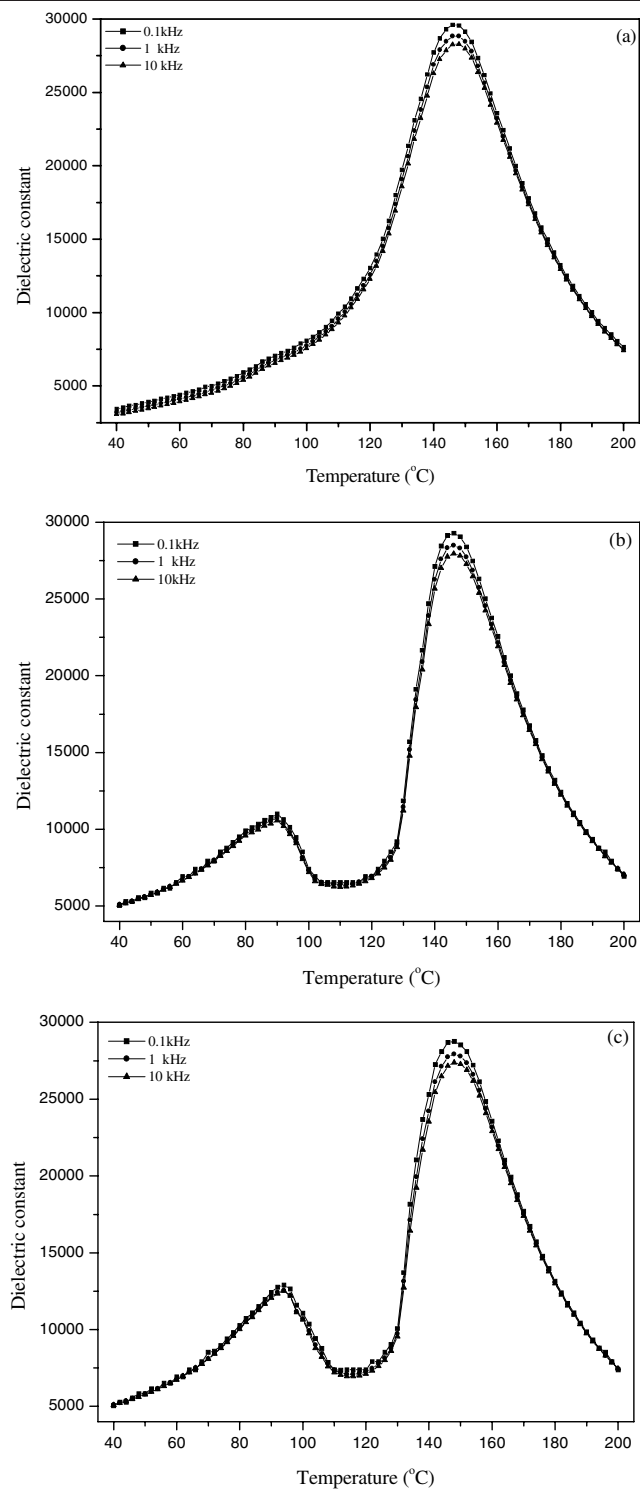


Figure 1. The dielectric constant as functions of temperature for (001)-oriented 0.7PMN-0.3PT single crystals in different frequency and poling conditions: (a) unpoled; (b) $E_{poling} = 4 \text{ kV cm}^{-1}$; (c) $E_{poling} = 13 \text{ kV cm}^{-1}$.

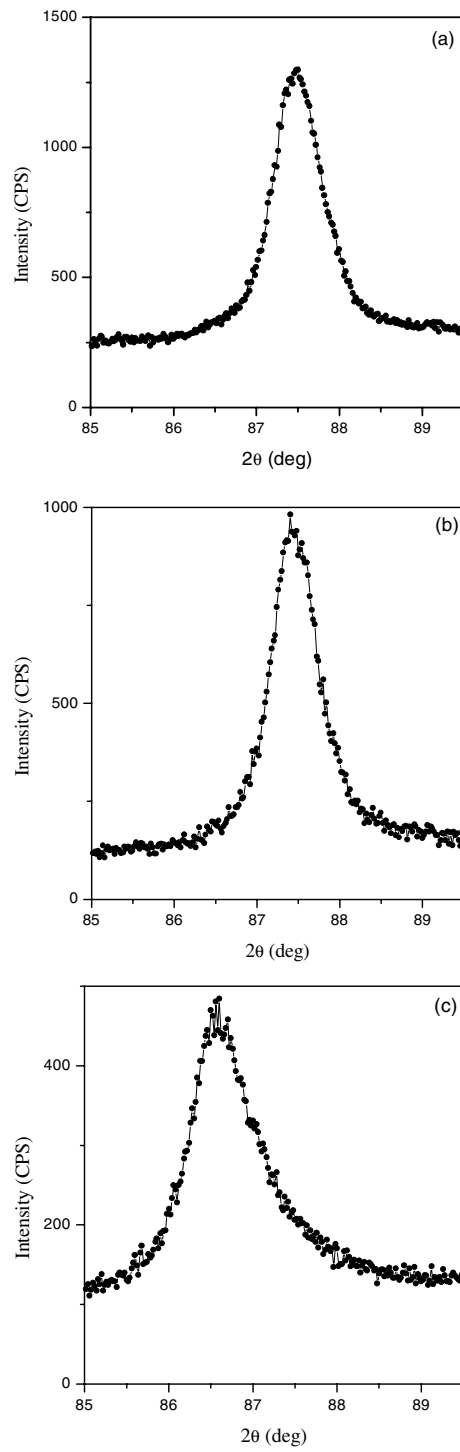


Figure 2. The (004) x-ray diffraction lines of 0.7PMN–0.3PT single crystals: (a) unpoled; (b) poled at $E_{poling} = 4 \text{ kV cm}^{-1}$; (c) poled at $E_{poling} = 13 \text{ kV cm}^{-1}$. All the measurements were at room temperature.

at half-maximum) angle of $\Delta 2\theta = 0.56^\circ$, which implies that a pseudocubic phase, FE_{SRO} , exists in the unpoled 0.7PMN–0.3PT single crystals. This is consistent with the results of the dielectric measurements. According to the Scherrer equation [18], the mean dimension of the microdomains can be estimated by using the broadening of the diffraction line. Comparison between figures 2(a) and (b) indicated that the mean dimension of microdomains of the unpoled sample is around 10 nm. The lattice parameter a of this form was calculated from the (400) line. It is equal to 0.402 nm, which is almost identical to the results of Singh and Pandey [19] ($a = 0.4023$ nm) and Zhang and Fang [20] ($a = 0.4019$ nm) for 0.7PMN–0.3PT ceramics also having the pseudocubic form. The existence of a rhombohedral ferroelectric state with short-range ordering, FE_{SRO} , is in agreement with the results given in [15] for unpoled single crystals with same composition, and can be explained by the effect of the internal random field [21] originating from compositional fluctuation and other defects, as shown clearly by HRTEM observation [22].

Figure 2(b) shows the (004) diffraction line of the sample poled at 4 kV cm^{-1} . The profile is also symmetric, with a diffraction angle equal to the unpoled one ($2\theta = 87.50^\circ$). But its FWHM ($\Delta 2\theta = 0.44^\circ$) is much narrower than that for the unpoled sample. This means that the crystal form does not change in this transition, while the FE_{LRO} (long-range-ordered rhombohedral ferroelectric) can be perfectly induced in the poled sample with $E_{\text{poling}} = 4 \text{ kV cm}^{-1}$. It is suggested that the effect of the random internal field can be overcome by an appropriate poling field. Furthermore, the metastable FE_{LRO} state can be locked even after the removal of the electric field in the room temperature. However, upon thermal cycling a FE_{LRO} -to- FE_{SRO} phase transition of this sample occurs at around 90°C . This phase transition can be regarded as a ‘defrozen process’ [23] and the temperature 90°C is similar to T_f [15, 22]. For the sample poled under $E_{\text{poling}} = 13 \text{ kV cm}^{-1}$, a quite different profile of the (004) diffraction line was observed, as shown in figure 2(c). Although the plots of the dielectric constant measurements, figures 1(b) and (c), are almost the same, the peak of the (400) profile was shifted to $2\theta = 86.60^\circ$. Thus the lattice parameter c of this form increases to 0.406 nm, which is even larger than $c_{\text{M}} = 0.405$ nm for the monoclinic phase, which is an intermediate phase near the MPB between the FE_{R} phase and the FE_{T} phase [14]. Recently, Noheda *et al* [24] indicated that the tetragonal phase could be induced by an electric field larger than 10 kV cm^{-1} applied along the [001] direction of PZN–4.5PT single crystal. Therefore, in our case it is reasonable to suggest that a fraction of the tetragonal ferroelectric state FE_{T} has been induced by the stronger applied field, although the polarization rotation from $\langle 111 \rangle$ to $\langle 001 \rangle$ may not be complete, as suggested by the asymmetric diffraction peak shown in figure 2(c). It is suggested that the volume of the unit cell of this sample remains constant with increasing electric field; on this basis, the lattice parameter a of the tetragonal form is equal to 0.400 nm.

In addition to the XRD experiments, our explanation is also supported by the measurements of the piezoelectric constant d_{33} . The value of d_{33} for the sample poled at $E_{\text{poling}} = 4 \text{ kV cm}^{-1}$ is higher than 1500 pC N^{-1} , but is decreased to 850 pC N^{-1} for the sample poled at $E_{\text{poling}} = 13 \text{ kV cm}^{-1}$. The additional poling at 13 kV cm^{-1} results in a phase transformation from the rhombohedral to the tetragonal phase, which reduces the contribution from the $\langle 111 \rangle$ polarization rotation.

In summary, these experiments indicate that the electric-field-induced phase transformation depends on the poling intensity for $\langle 001 \rangle$ -oriented 0.7PMN–0.3PT single crystals. A weaker poling intensity ($E_{\text{poling}} = 4 \text{ kV cm}^{-1}$) can overcome the effect of a random internal field and transform the phase from FE_{SRO} to FE_{LRO} . But the rhombohedral ferroelectric-to-tetragonal ferroelectric phase transformation originating from the rotation from $\langle 111 \rangle$ to $\langle 001 \rangle$ polarization can only be induced by a stronger poling intensity ($E_{\text{poling}} = 13 \text{ kV cm}^{-1}$). The sample poled at $E_{\text{poling}} = 4 \text{ kV cm}^{-1}$ shows a larger piezoelectric effect.

This work was supported by the National Natural Science Foundation of China grant no 59995522. The authors would like to thank Dr Newnham, Dr Chen Jie and Dr Fang Fei for helpful discussions.

References

- [1] Kuwata J, Uchino K and Nomura S 1981 *Ferroelectrics* **37** 579
- [2] Kuwata J, Uchino K and Nomura S 1982 *Japan. J. Appl. Phys.* **21** 1298
- [3] Service R F 1997 *Science* **275** 1878
- [4] Park S-E and Shrout T R 1997 *IEEE Trans. Ultrason. Ferroelectr. Freq. Control* **44** 1140
- [5] Park S-E and Shrout T R 1997 *J. Appl. Phys.* **82** 1804
- [6] Park S-E and Shrout T R 1997 *Mater. Res. Innovat.* **1** 20
- [7] Fu H and Cohen R E 2000 *Nature* **403** 281
- [8] Noheda B, Cox D E, Shirane G, Gonzalo J A, Cross L E and Park S-E 1999 *Appl. Phys. Lett.* **74** 2059
- [9] Noheda B, Gonzalo J A, Cross L E, Guo R, Park S-E, Cox D E and Shirane G 1999 *Phys. Rev. B* **61** 8687
- [10] Noheda B, Cox D E, Shirane G, Guo R, Jones B and Cross L E 2001 *Phys. Rev. B* **63** 014103
- [11] Durbin M K, Jacobs E W, Hicks J C and Park S-E 1999 *Appl. Phys. Lett.* **74** 2848
- [12] Durbin M K, Hicks J C, Park S-E and Shrout T R 2000 *J. Appl. Phys.* **87** 8159
- [13] Noheda B, Cox D E, Shirane G, Park S-E, Cross L E and Zhong Z 2001 *Phys. Rev. Lett.* **86** 3891
- [14] Ye Z-G, Noheda B, Dong M, Cox D E and Shirane G 2001 *Phys. Rev. B* **64** 184114
- [15] Viehland D, Powers J, Cross L E and Li J F 2001 *Appl. Phys. Lett.* **78** 3508
- [16] Lu Y, Jeong D-Y, Cheng Z-Y, Zhang Q M, Luo H S, Yin Z W and Viehland D 2001 *Appl. Phys. Lett.* **78** 3109
- [17] Luo H W, Xu G S, Xu H, Wang P and Yin Z W 2000 *Japan. J. Appl. Phys.* **39** 5581
- [18] Cullity B D 1978 *Elements of X-ray Diffraction* (Reading, MA: Addison-Wesley) p 284
- [19] Singh A K and Pandey D 2001 *J. Phys.: Condens. Matter* **13** L931
- [20] Zhang X W and Fang F 1999 *J. Mater. Res.* **14** 4581
- [21] Kleemann W 1993 *Int. J. Mod. Phys. B* **7** 2469
- [22] Jin H, Zhu J, Miao S, Zhang X W and Cheng Z 2001 *J. Appl. Phys.* **89** 5048
- [23] Gui H, Gu B and Zhang X W 1995 *Phys. Rev. B* **52** 3135
- [24] Noheda B, Zhong Z, Cox D E, Shirane G, Park S-E and Rehrig P 2002 *Preprint cond-mat/0201182*